

# A novel hexaaza macrocycle with methylenephosphonate pendant arms: a potential useful chelate for biomedical applications†

S. W. Annie Bligh,<sup>\*,a</sup> Nick Choi,<sup>a</sup> Carlos F. G. C. Geraldles,<sup>b</sup> Stefan Knoke,<sup>a</sup> Mary McPartlin,<sup>a</sup> Mahesh J. Sanganeer<sup>a</sup> and Thomas M. Woodroffe<sup>a</sup>

<sup>a</sup> School of Applied Chemistry, University of North London, Holloway Road, London, UK N7 8DB

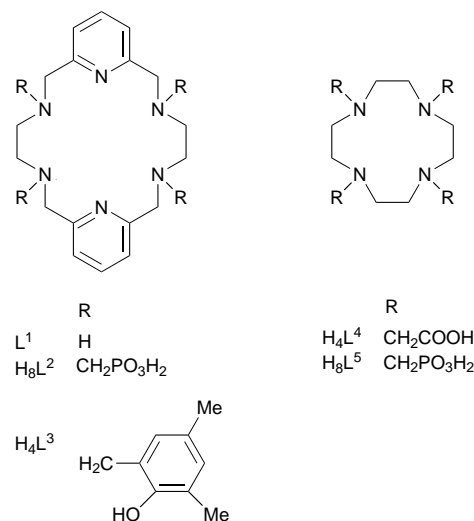
<sup>b</sup> Department of Biochemistry and Centre of Neurosciences, Faculty of Science and Technology, University of Coimbra, 3049 Coimbra Codex, Portugal

A new 18-membered hexaaza macrocyclic ligand with four pendant methylenephosphonates has been synthesized *via* the Mannich reaction. The protonation behaviour of this macrocycle has been followed by <sup>31</sup>P and <sup>1</sup>H NMR spectroscopy. The initial protonation pattern of the N-functionalised macrocycle is rather like its corresponding macrocyclic amine. The proton NMR spectrum of its lanthanum(III) complex in aqueous solution indicates that the complex adopts only one of the five possible conformations, either *SSSS* or *RRRR*. The crystal structure of the novel macrocyclic ligand shows an extended hydrogen-bonded structure in its solid state. The macrocycle has an unusual conformation with the pendants alternating 'up' and 'down' round the ring. The La<sup>III</sup> complex has a unique ten-co-ordinate geometry with all pendant arms co-ordinated to the La<sup>III</sup> ion which is in the plane of the six macrocyclic nitrogen donors.

Stable metal chelates of polyfunctional macrocyclic ligands have attracted considerable interest especially in radiopharmaceutical and biomedical NMR applications. The complexation properties of polyaza macrocycles are governed mainly by the macrocyclic ring size. N-Functionalization of these macrocycles can enhance their metal-ion selectivity and the stability of metal complexes depending on the co-ordination properties of the pendant arms.

Polyaza macrocycles with acetate pendant arms such as 1,4,7,10-tetraazacyclododecane-*N,N',N'',N'''*-tetraacetic acid ( $H_4L^4$ ) have been shown to form stable complexes with the trivalent lanthanide cations in aqueous solution.<sup>1</sup> In 1989 the *N*-methyl-D-glucamine [1-deoxy-1-(methylamino)-D-glucitol] salt of [Gd( $L^4$ )(H<sub>2</sub>O)]<sup>−</sup> (DOTAREM) became the second magnetic resonance imaging (MRI) contrast agent available on the pharmaceutical market, and is an alternative to [Gd(DTPA)(H<sub>2</sub>O)]<sup>2−</sup> (Magnevist) ( $H_5$ DTPA = diethylenetriaminepentaacetic acid). The lanthanide complexes of a second related tetraaza macrocycle with methylenephosphonate pendant arms, 1,4,7,10-tetraazacyclododecane-*N,N',N'',N'''*-1,4,7,10-tetrakis(methylenephosphonic acid) ( $H_8L^5$ ), have been studied in some detail with regard to their solution and magnetic properties,<sup>2–4</sup> and as high resolution NMR shift reagents for proteins,<sup>5,6</sup> as well as shift reagents for *in vivo* <sup>23</sup>Na NMR spectroscopy.<sup>7,8</sup>

Recently we have reported the synthesis of a gadolinium complex of a novel 18-membered hexaaza macrocycle with 2-hydroxy-3,5-dimethylbenzyl pendant arms,  $H_4L^3$ , and its potential as an MRI contrast agent.<sup>9</sup> We have now extended this work to the synthesis of a new ligand in which four methylenephosphonate functional groups have been incorporated on the hexaaza macrocycle. The structure of this novel macrocyclic ligand, 3,6,14,17,23,24-hexaazatricyclo[17.3.1.1<sup>8,12</sup>]tetracosal(23),8,10,12(24),19,21-hexaene-3,6,14,17-tetrakis(methylenephosphonic acid) ( $H_8L^2$ ) and of its lanthanum(III) complex have been established by X-ray crystallography. It is anticipated that the lanthanide complexes of this potentially decadentate macrocyclic ligand will have biological applications including their use as MRI contrast agents (Gd<sup>III</sup>, Dy<sup>III</sup>), NMR shift reagents (Dy<sup>III</sup>, Tm<sup>III</sup>) and bone palliative agents



(Sm<sup>III</sup>). The ligand itself,  $H_8L^2$ , may be used as a metal-ion selective probe for biological systems monitored by <sup>31</sup>P NMR spectroscopy. In this work protonation of  $H_8L^2$  has been investigated by <sup>31</sup>P and <sup>1</sup>H NMR spectroscopy, and a comparative study of the NMR spectroscopic data obtained is made with the  $H_8L^5$  ligand.<sup>10</sup>

## Results and Discussion

### Synthesis

The macrocyclic ligand  $H_8L^2$  is the first 18-membered hexaaza macrocycle containing four methylenephosphonate pendant arms to be prepared. The optimum reaction condition was the use of a double to triple excess of phosphorous acid and formaldehyde and a 24 h period of reflux. Pure material was obtained by dissolving the crude product in dilute HCl and recrystallising it from ethanol. The substitution of all the amino hydrogen atoms was shown by the absence of the N–H bands at 3285 cm<sup>−1</sup>, and the strong bands at 1158 and 1074 cm<sup>−1</sup> corresponding to the phosphoryl confirmed the successful synthesis of the ligand  $H_8L^2$ . The mass spectrum of the macrocyclic ligand and  $H_8L^5$  has a parent ion at *m/z* 703 corresponding to [*M*+H]<sup>+</sup>

† Based on the presentation given at Dalton Discussion No. 2, 2nd–5th September 1997, University of East Anglia, UK.

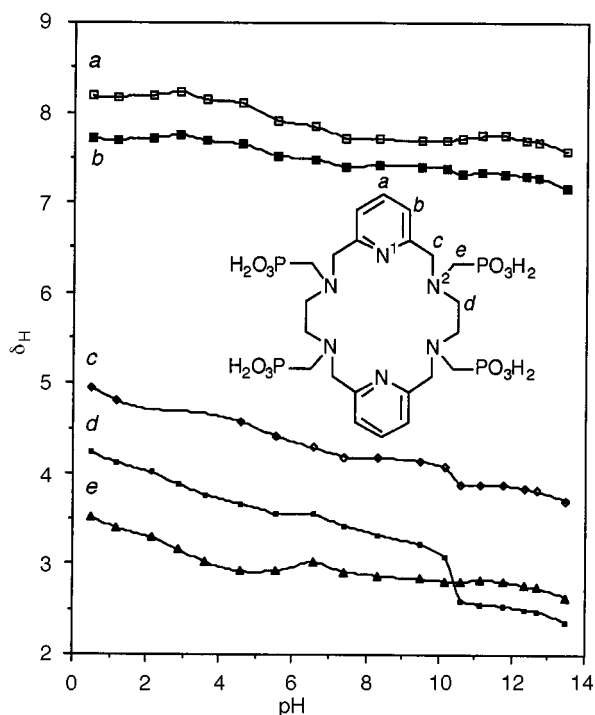


Fig. 1 The  $^1\text{H}$  NMR chemical shifts of  $\text{H}_8\text{L}^2$  recorded as a function of solution pH. Chemical shift assignments are shown

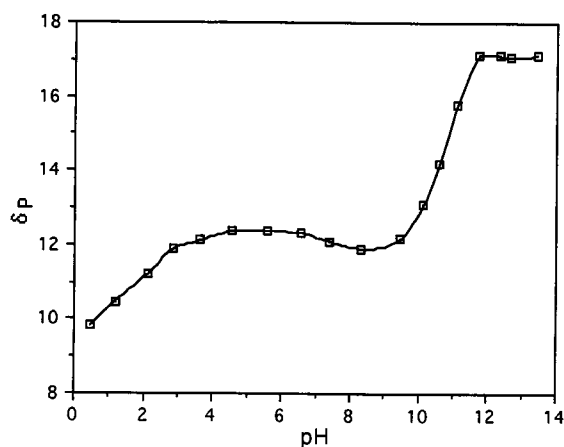


Fig. 2 The  $^{31}\text{P}$  NMR chemical shifts of  $\text{H}_8\text{L}^2$  recorded as a function of solution pH

and a base peak at  $m/z$  623 indicating that one  $\text{HPO}_3$  is fragmented.

### NMR spectroscopic studies

The protonation sequence of the ligand  $\text{H}_8\text{L}^2$  was followed by the pH dependence of its  $^1\text{H}$  and  $^{31}\text{P}$  chemical shifts in aqueous solution (Figs. 1 and 2). All spectra showed single resonances for each magnetically equivalent group of nuclei over the entire range of pH, displaying a rapid exchange process between all protonated species. The initial protonation steps of ligand  $\text{H}_8\text{L}^2$  are compared to the data obtained for  $\text{L}^1$  reported by Jackels and co-workers.<sup>11</sup> Following the microscopic protonation interpretation procedure of Sudmeier and Reilly,<sup>12</sup> we can conclude that the protonation shift of protons  $d$  reflect the protonation fraction at the four amine nitrogens  $\text{N}^2$  ( $f_2$ ), the protonation shift of  $a$  is proportional to the protonation fraction at the two pyridine nitrogens at  $\text{N}^1$  ( $f_1$ ) while the difference of protonation shift of protons  $d$  and  $e$  is proportional to the protonation fraction at the phosphonate group ( $f_p$ ). Using the protonation curves for  $\text{L}^1$  of the literature,<sup>11</sup> we could obtain values  $f_1 = 0.11$  and  $f_2 = 0.44$  for the  $[\text{H}_2\text{L}^1]^{2+}$  form, using shielding constants  $C_N = 1.12$  for protonation of an N atom at the  $\alpha$  position and

$C_N = 0.26$  for protonation of N at the  $\beta$  position. For this ligand, the pH range between 8.5 and 7.0 shows another protonation, with  $f_1 = 0.11$  and  $f_2 = 0.69$  for  $n = 3$ , and between pH 7.0 and 5.0,  $f_1 = 0.21$  and  $f_2 = 0.89$  for  $n = 4$  ( $n$  = number of equivalents of acid added to the fully unprotonated form). Thus, in ligand  $\text{L}^1$ , the protonation of the pyridine nitrogens down to pH 5.0 is much lower than the amine nitrogens.

In the case of our ligand  $\text{H}_8\text{L}^2$ , the first protonation step, in the range pH 11–9, as shown by the shifts of protons  $c$  and  $d$ , is quite similar to that observed for  $\text{L}^1$ . However, due to the influence of the pendant phosphonate arms, the first two protonation constants are displaced towards higher values (above 10) and the value of  $f_2$  is even higher relative to  $f_1$ , when compared with the case of  $\text{L}^1$ . Thus, the amine nitrogens  $\text{N}^2$  in  $\text{H}_8\text{L}^2$  are even more basic than those in  $\text{L}^1$ . The second protonation step, between pH 9 and 7 ( $n = 3$ ) corresponds again to a predominant protonation at  $\text{N}^2$ , as shown by the  $c$  and  $d$  proton shifts. The third protonation step, between pH 7 and 4 ( $n = 4$ ) shows that the fourth proton has a slight preference for  $\text{N}^1$  versus  $\text{N}^2$ . Finally, between pH 4 and 1,  $\text{N}^1$  is again negligibly protonated, while  $\text{N}^2$  and the phosphonate oxygens are protonated steadily, as shown by the shifts of protons  $c$ ,  $d$  and  $e$ , respectively.

In contrast to the insensitivity of the  $\text{N}^1$  protonation of the pyridine nitrogen observed in  $\text{L}^1$ , the total protonation shift of protons  $a$  is 0.61 ppm and of protons  $b$  is 0.55 ppm in the range pH 0.5–13.5 of  $\text{H}_8\text{L}^2$ . This supports a higher participation of protonation of pyridine nitrogens, which is reflected in the large increase of  $f_1$  observed in the change of  $n = 3$  to  $n = 4$ . The proton shifts of the  $\text{CH}_2\text{P}$  groups (protons  $e$ ) are relatively unaffected by  $\text{N}^2$  protonation between pH 12 and 9.5, possibly due to complexation of  $\text{Na}^+$  ion by the phosphonate oxygen, as observed before for  $\text{H}_8\text{L}^5$ .<sup>10</sup>

The  $^{31}\text{P}$  NMR chemical shifts versus pH titration curve (Fig. 2) shows a large and rather sharp upfield shift during the first protonation step of  $\text{H}_8\text{L}^2$  in the range pH 12–9.5 ( $n = 2$ ). This may be due in part to the complexation of  $\text{Na}^+$  by the macrocycle, which has been observed for other tri- and tetra-aza macrocyclic methylenephosphonate systems using NaOD as a titrant.<sup>10,13</sup> The gradual increase of the  $^{31}\text{P}$  shift from pH 8.3 to 6.0 indicates that the phosphonate oxygens are forming internal hydrogen bonds with the protonated ring amine nitrogens and there is evidence of this in the solid state [Fig. 4(a)]. The formation of this rather rigid structure is reflected in a considerable broadening of the  $^{31}\text{P}$  signal observed below pH 6.5 indicating slowing down of the interconversion of the various possible hydrogen-bonded structures [Fig. 4(a)]. Again, such a situation has been observed before for  $\text{H}_8\text{L}^5$  in solution and there is confirmation of intramolecular H-bonding in the crystal structure.<sup>14</sup> Finally the upfield shift of the  $^{31}\text{P}$  resonance at a pH below 5.0 reflects protonation of the phosphonate oxygens, with gradual breaking down of the hydrogen bond. The quantitative deduction of the protonation sequence of  $\text{H}_8\text{L}^2$  is rather difficult and can only be achieved after a thorough potentiometric study determining the macroscopic protonation constants of the ligand.

The macrocyclic chelate  $\text{H}_8\text{L}^2$  forms a 1:1 stable complex with  $\text{La}^{\text{III}}$  ions. The  $^1\text{H}$  NMR spectrum of the neutral  $[\text{La}(\text{H}_5\text{L}^2)]$  complex together with its solid state characterisation suggests that the ligand adopts only one of the five possible configurations, i.e. the SSSS or RRRR configuration. The proton NMR spectrum consists of a triplet and a doublet centred at  $\delta$  7.75 and 7.26 ( $^3J_{\text{HH}} = 7.5$  Hz) corresponding to the pyridine protons. The pyridyl protons,  $c$  and  $c'$ , yield an AB pattern at  $\delta$  3.70 and 4.69 with  $^2J_{\text{HH}} = -10.9$  Hz and similarly the ethylenic protons,  $d$  and  $d'$ , give an AB pattern at  $\delta$  3.28 and 3.50 ( $^2J_{\text{HH}} = -15.3$  Hz) consistent with the ligand maintaining its four-fold symmetry upon complex formation in solution. This indicates that the five-membered rings formed by  $\text{La}^{\text{III}}$  and the ethylenediamine unit at the  $\text{N}^2$  atom are flexible, with a fast interconversion in solution between  $\delta$  and  $\lambda$  configurations. In

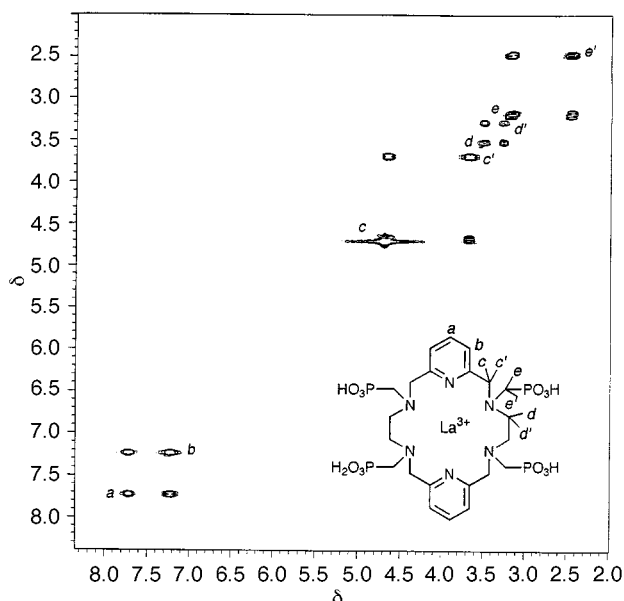


Fig. 3 Two-dimensional COSY spectrum of  $[\text{La}(\text{H}_5\text{L}^2)]$  at pH 8.2

contrast,  $[\text{La}(\text{L}^5)]^{5-}$  has a rigid tetraaza macrocyclic ring structure and the four ethylenic protons give a first-order AA'XX' spectrum.<sup>3</sup> The methylene phosphonate protons, *e* and *e'*, show two multiplets ( $^3J_{\text{HP}} = 7.50$  and  $17.0$  Hz), consisting of the AB part of an ABX spectrum (X is the  $^{31}\text{P}$  nucleus). The assignments of the proton signals and the verification of the geminal couplings were based upon a two-dimensional homonuclear correlation (COSY) spectrum (Fig. 3). The  $^{31}\text{P}$  NMR spectrum of the  $[\text{La}(\text{H}_5\text{L}^2)]$  complex shows a complexation shift of  $+10.8$  ppm which is comparatively larger than the shift obtained in  $[\text{La}(\text{L}^5)]^{5-}$  ( $+7.2$  ppm).

### Crystal structure

The crystal structures of the free ligand  $\text{H}_8\text{L}^2$  and its lanthanum complex  $[\text{La}(\text{H}_5\text{L}^2)]$  have been established by X-ray analysis. The molecular structure of the 18-membered hexaaza macrocyclic free ligand  $\text{H}_8\text{L}^2$  is shown in Fig. 4(a); selected bond lengths and angles are listed in Table 1. The overall conformation of the free hexaaza macrocycle is slightly twisted (dihedral angle between the dimethylpyridyl groups  $23.7^\circ$ ), but is not folded in contrast to related hexaaza macrocycles which all have markedly stepped conformations. For example the pyridyl units, in the analogous tetramethyl- $\text{H}_4\text{L}^3$  with 2-hydroxy-3,5-dimethylbenzyl pendant arms were almost perpendicular to the best plane through the great ring the dihedral angle being  $98.3^\circ$  as can be seen in Fig. 4(b).<sup>9</sup> The difference in conformation arises from the unusual orientation of the pendant arms in  $\text{H}_8\text{L}^2$ , the phosphonate pendants associated with one diaminomethyl-enepyridyl group lying on opposite sides of the macrocycle ring, so that they alternate 'up' and 'down' round the ring [Fig 4(a)], whereas for other derivatised hexaaza macrocycles they occur in pairs 'above' and 'below' the ring.<sup>9</sup> The only other aza macrocycle with four pendant phosphonate arms to have been structurally characterised is the tetraaza macrocycle  $\text{H}_8\text{L}^5$  in which two diagonally opposite phosphonate groups lie above the macrocycle ring and two extend sideways.<sup>14</sup>

The P–O bond lengths fall into two groups, one bond on each phosphonate group being significantly longer than the other two, indicating an anionic mono deprotonated  $\text{PO}_3\text{H}^-$  formulation. The shorter P–O lengths are in the range  $1.48\text{--}1.52(2)$  Å (mean  $1.50$  Å) within the range observed for P–O bonds in aminophosphonates,<sup>15,16</sup> and the four longer P–O bonds are in the range  $1.57\text{--}1.59(2)$  Å and may be assumed to be protonated. From this evidence it may be deduced that the molecule exists in zwitterionic form with four protonated amine groups; the N–C bond lengths are in the range  $1.49\text{--}1.52(2)$  (mean  $1.51$  Å) con-

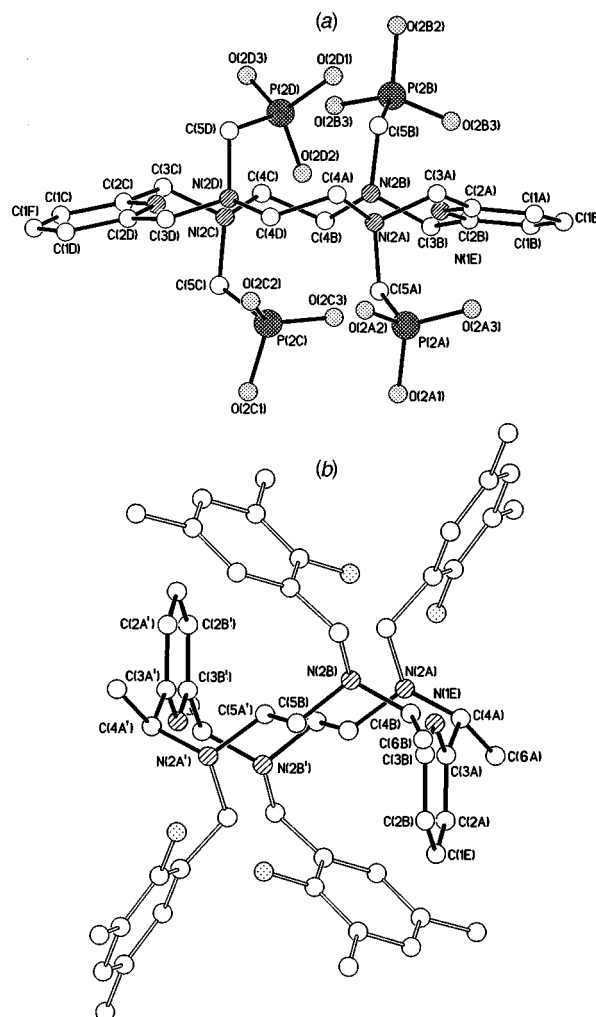


Fig. 4 (a) The molecular structure of  $\text{H}_8\text{L}^2$  showing the unusual arrangement of the phosphonate pendant arms, and the conformation of the macrocycle which is preorganised for complexation. The unprotonated oxygen atom O(2D2) is close to the centre of the macrocycle and in hydrogen-bonded contact with the calculated positions of three amino protons [ $\text{H}(\text{N}2\text{A})$   $2.00$ ,  $\text{H}(\text{N}2\text{B})$   $2.01$ ,  $\text{H}(\text{N}2\text{C})$   $1.92$  Å]; the fourth amino proton appears to be H-bonded to a second unprotonated oxygen atom [ $\text{O}(\text{2C}2) \cdots \text{H}(\text{N}2\text{D})$   $2.05$  Å]. (b) Reported structure of tetramethyl- $\text{H}_4\text{L}^3$  showing the step conformation of the macrocycle<sup>9</sup>

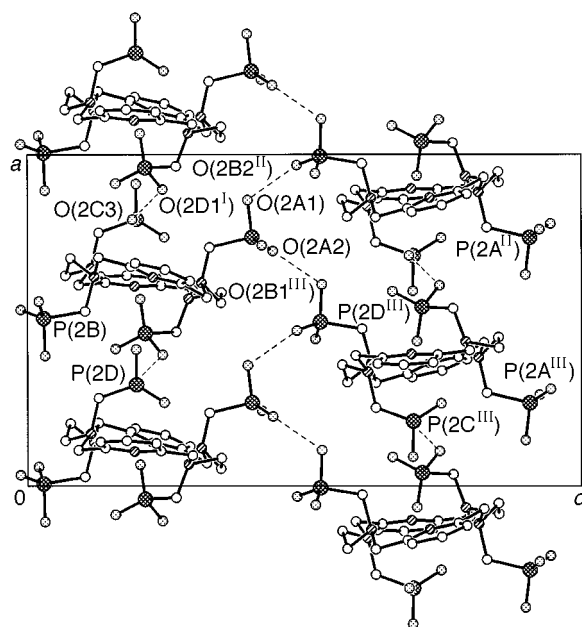
sistent, although at a low significance, with the characteristic slight lengthening observed for N–C bonds from protonated nitrogen atoms in other aminophosphonates.<sup>13,16</sup>

Two of the pendant arms are wrapped across the macrocycle [P(2C) and P(2D)] and two are extended outwards; an unprotonated oxygen atom of a wrapping pendant, O(2D2), lies a short distance above the macrocycle cavity and is in very close proximity to the calculated H atom positions on three of the amino groups [ $\text{H}(\text{N}2\text{A})$   $2.00$ ,  $\text{H}(\text{N}2\text{B})$   $2.01$ ,  $\text{H}(\text{N}2\text{C})$   $1.92$  Å] which is consistent with some form of H-bonding interaction between these atoms. The fourth amino proton is more remote [ $\text{O}(\text{2D}2) \cdots \text{H}(\text{N}2\text{D})$   $2.23$  Å] but appears to make an H-bonding contact with an unprotonated oxygen atom from the second 'wrapped round' pendant arm [ $\text{O}(\text{2C}2) \cdots \text{H}(\text{N}2\text{D})$   $2.05$  Å]. Three of four oxygen atoms assigned to the P(OH) groups make extremely short contacts with unprotonated phosphonate oxygen atoms of neighbouring molecules ( $2.50\text{--}2.57$  Å) indicating very strong intermolecular H-bonding (Fig. 5), and the fourth is hydrogen bonded to a full occupancy water molecule [ $\text{O}(\text{2C}2) \cdots \text{O}(6)$   $2.63$  Å].

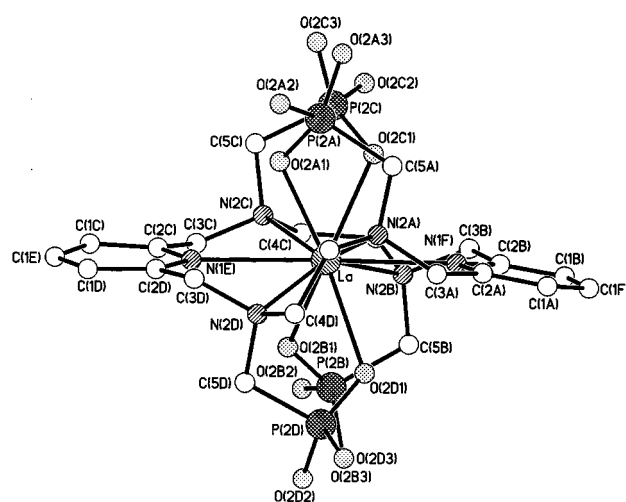
The X-ray structure analysis of  $[\text{La}(\text{H}_8\text{L}^2)]$  confirms the SSSS/RRRR conformation of the macrocycle indicated by the  $^1\text{H}$  NMR studies; both enantiomers are present in the crystal,

**Table 1** Selected bond lengths (Å) and angles (°) for  $H_8L^2$ 

P(2A)–O(2A2)	1.48(2)	P(2A)–O(2A3)	1.51(2)
P(2A)–O(2A1)	1.58(2)	P(2A)–C(5A)	1.84(2)
P(2B)–O(2B2)	1.52(2)	P(2B)–O(2B3)	1.51(2)
P(2B)–O(2B1)	1.59(1)	P(2B)–C(5B)	1.85(2)
P(2C)–O(2C2)	1.49(2)	P(2C)–O(2C3)	1.52(1)
P(2C)–O(2C1)	1.58(2)	P(2C)–C(5C)	1.84(2)
P(2D)–O(2D3)	1.48(2)	P(2D)–O(2D2)	1.52(1)
P(2D)–O(2D1)	1.57(2)	P(2D)–C(5D)	1.87(2)
N(2A)–C(5A)	1.52(2)	N(2A)–C(4A)	1.50(2)
N(2A)–C(3A)	1.51(2)	C(4A)–C(4D)	1.56(2)
N(2B)–C(4B)	1.50(2)	N(2B)–C(5B)	1.51(2)
N(2B)–C(3B)	1.52(2)	C(4B)–C(4C)	1.53(2)
N(2C)–C(4C)	1.49(2)	N(2C)–C(3C)	1.50(2)
N(2C)–C(5C)	1.52(2)	N(2D)–C(5D)	1.51(2)
N(2D)–C(3D)	1.49(2)	N(2D)–C(4D)	1.50(2)
O(2A2)–P(2A)–O(2A3)	114.5(11)	O(2A2)–P(2A)–O(2A1)	111.7(11)
O(2A3)–P(2A)–O(2A1)	112.1(10)	O(2A2)–P(2A)–C(5A)	111.9(10)
O(2A3)–P(2A)–C(5A)	108.8(10)	O(2A1)–P(2A)–C(5A)	96.5(9)
O(2B2)–P(2B)–O(2B3)	117.8(10)	O(2B2)–P(2B)–O(2B1)	108.6(9)
O(2B3)–P(2B)–O(2B1)	112.1(10)	O(2B2)–P(2B)–C(5B)	108.3(9)
O(2B3)–P(2B)–C(5B)	109.7(10)	O(2B1)–P(2B)–C(5B)	98.6(9)
O(2C2)–P(2C)–O(2C3)	117.6(10)	O(2C2)–P(2C)–O(2C1)	111.6(9)
O(2C3)–P(2C)–O(2C1)	108.4(9)	O(2C2)–P(2C)–C(5C)	108.9(9)
O(2C3)–P(2C)–C(5C)	108.8(10)	O(2C1)–P(2C)–C(5C)	100.2(9)
O(2D3)–P(2D)–O(2D2)	113.3(9)	O(2D3)–P(2D)–O(2D1)	111.2(9)
O(2D2)–P(2D)–O(2D1)	112.3(9)	O(2D3)–P(2D)–C(5D)	110.2(10)
O(2D2)–P(2D)–C(5D)	107.0(8)	O(2D1)–P(2D)–C(5D)	102.0(10)
N(2A)–C(5A)–P(2A)	117.7(13)	N(2B)–C(5B)–P(2B)	117.5(14)
N(2C)–C(5C)–P(2C)	115.4(14)	N(2D)–C(5D)–P(2D)	109.8(14)
C(5A)–N(2A)–C(4A)	114(2)	C(5A)–N(2A)–C(3A)	111.3(14)
C(4A)–N(2A)–C(3A)	107.4(14)	C(4B)–N(2B)–C(5B)	115(2)
C(4B)–N(2B)–C(3B)	108.2(14)	C(5B)–N(2B)–C(3B)	111(2)
C(4C)–N(2C)–C(3C)	105.5(14)	C(4C)–N(2C)–C(5C)	116(2)
C(3C)–N(2C)–C(5C)	112(2)	C(5D)–N(2D)–C(3D)	111(2)
C(5D)–N(2D)–C(4D)	113(2)	C(3D)–N(2D)–C(4D)	108(2)

**Fig. 5** The two-dimensional polymer generated by hydrogen bonding between protonated and unprotonated phosphonate oxygen atoms in the solid-state structure of  $H_8L^2$  viewed down the  $b$  axis. The molecules form stacks parallel to the  $a$  axis [O(2C3)⋯O(2D1<sup>I</sup>) 2.49 Å; I 0.5 +  $x$ , 0.5 –  $y$ ,  $z$ ]; the parallel columns are further linked by hydrogen bonding [O(2A1)⋯O(2B2<sup>II</sup>) 2.57 Å; II 1.5 –  $x$ ,  $y$ , 0.5 +  $z$ ] and [O(2A2)⋯O(2B1<sup>III</sup>) 2.50 Å; III 1 –  $x$ , 0.5 –  $y$ , 0.5 +  $z$ ]

related by the inversion of the  $n$ -glide planes, and the SSSS conformation is illustrated in Fig. 6; selected bond lengths and angles are listed in Table 2. The lanthanum ion has the irregular ten-co-ordinate geometry derived from four oxygen atoms of the four phosphonate pendant arms and six nitrogen atoms of

**Fig. 6** The molecular structure of the ten-co-ordinated hexaaza macrocyclic complex  $[La(H_8L^2)]$  showing the co-ordination of four pendant arms

the 18-membered hexaaza macrocycle. The  $[La(H_8L^2)]$  complex is thus the first lanthanide macrocyclic complex with four co-ordinated pendant arms. For example, the gadolinium complex of  $H_8L^3$ ,  $[Gd(H_8L^3)(NO_3)]^+$  with the same 18-membered hexaaza macrocyclic framework, has only one of its four 2-hydroxy-3,5-dimethylbenzyl pendant arms co-ordinated to the metal ion and the other three pendant arms radiate out away from the metal centre.<sup>9</sup>

It has been observed previously that in hexaaza macrocyclic complexes two types of conformation are possible, which may be defined relative to a hypothetical planar arrangement.<sup>17</sup> In a 'twist-wrap' conformation, the macrocyclic ligand wraps round the metal ion by a twisting of the pyridyl bridgehead units rel-

**Table 2** Selected bond lengths (Å) and angles (°) for [La(H<sub>5</sub>L<sup>2</sup>)]

La–O(2A1)	2.556(8)	La–O(2B1)	2.517(9)
La–O(2C1)	2.576(9)	La–O(2D1)	2.579(8)
La–N(1E)	2.731(10)	La–N(1F)	2.694(10)
La–N(2A)	2.824(10)	La–N(2B)	2.780(10)
La–N(2C)	2.793(11)	La–N(2D)	2.813(11)
O(2A1)–P(2A)	1.493(9)	O(2B1)–P(2B)	1.492(9)
O(2C1)–P(2C)	1.506(9)	O(2D1)–P(2D)	1.498(10)
P(2A)–O(2A3)	1.504(9)	P(2A)–O(2A2)	1.583(9)
P(2B)–O(2B2)	1.587(9)	P(2C)–O(2C2)	1.534(9)
P(2C)–O(2C3)	1.558(9)	P(2D)–O(2D3)	1.518(10)
P(2D)–O(2D2)	1.568(9)	P(2B)–O(2B3)	1.526(9)
P(2A)–C(5A)	1.810(13)	P(2B)–C(5B)	1.815(14)
P(2D)–C(5D)	1.799(14)	P(2C)–C(5C)	1.807(12)
N(2A)–C(5A)	1.45(2)	N(2A)–C(3A)	1.46(2)
N(2A)–C(4A)	1.52(2)	N(2C)–C(3C)	1.48(2)
N(2C)–C(5C)	1.50(2)	N(2C)–C(4C)	1.52(2)
N(2B)–C(5B)	1.47(2)	N(2B)–C(3B)	1.48(2)
N(2B)–C(4B)	1.51(2)	N(2D)–C(5D)	1.47(2)
N(2D)–C(3D)	1.48(2)	N(2D)–C(4D)	1.51(2)
O(2B1)–La–O(2A1)	139.2(3)	O(2B1)–La–O(2C1)	119.6(3)
O(2A1)–La–O(2C1)	68.9(3)	O(2B1)–La–O(2D1)	69.3(3)
O(2A1)–La–O(2D1)	132.6(3)	O(2C1)–La–O(2D1)	139.9(3)
O(2B1)–La–N(1F)	111.6(3)	O(2A1)–La–N(1F)	108.8(3)
O(2C1)–La–N(1F)	72.1(3)	O(2D1)–La–N(1F)	68.7(3)
O(2B1)–La–N(1E)	71.5(3)	O(2A1)–La–N(1E)	68.8(3)
O(2C1)–La–N(1E)	111.9(3)	O(2D1)–La–N(1E)	107.9(3)
O(2B1)–La–N(2B)	65.6(3)	O(2B1)–La–N(2C)	64.9(3)
O(2A1)–La–N(2C)	88.2(3)	O(2C1)–La–N(2C)	65.8(3)
O(2D1)–La–N(2C)	133.9(3)	O(2A1)–La–N(2B)	133.3(3)
O(2C1)–La–N(2B)	64.9(3)	O(2D1)–La–N(2B)	89.4(3)
O(2B1)–La–N(2D)	92.7(3)	O(2A1)–La–N(2D)	76.2(3)
O(2C1)–La–N(2D)	143.9(3)	O(2D1)–La–N(2D)	63.5(3)
O(2B1)–La–N(2A)	144.9(3)	O(2A1)–La–N(2A)	63.3(3)
O(2C1)–La–N(2A)	92.0(3)	O(2D1)–La–N(2A)	76.7(3)
N(1F)–La–N(1E)	173.3(3)	N(1F)–La–N(2B)	62.7(3)
N(1E)–La–N(2B)	123.7(3)	N(1F)–La–N(2C)	124.5(3)
N(1E)–La–N(2C)	62.1(3)	N(2B)–La–N(2C)	67.5(3)
N(1F)–La–N(2D)	112.7(3)	N(1E)–La–N(2D)	60.8(3)
N(2B)–La–N(2D)	150.5(3)	N(2C)–La–N(2D)	122.7(3)
N(1F)–La–N(2A)	61.2(3)	N(1E)–La–N(2A)	112.6(3)
N(2B)–La–N(2A)	123.5(3)	N(2C)–La–N(2A)	149.4(3)
N(2D)–La–N(2A)	63.8(3)	C(2C)–N(1E)–La	120.6(9)
C(2D)–N(1E)–La	121.4(8)	C(2B)–N(1F)–La	122.5(8)
C(2A)–N(1F)–La	120.2(8)	C(3A)–N(2A)–La	108.4(7)
C(5A)–N(2A)–La	103.8(7)	C(3C)–N(2C)–La	111.6(8)
C(4A)–N(2A)–La	112.5(8)	C(4C)–N(2C)–La	111.4(7)
C(5C)–N(2C)–La	105.7(7)	C(3B)–N(2B)–La	110.2(7)
C(5B)–N(2B)–La	107.2(8)	O(2A1)–P(2A)–O(2A2)	108.3(5)
C(4B)–N(2B)–La	112.9(7)	O(2A1)–P(2A)–C(5A)	105.5(5)
O(2A1)–P(2A)–O(2A3)	117.8(5)	O(2A2)–P(2A)–C(5A)	108.9(6)
O(2A3)–P(2A)–O(2A2)	107.5(5)	O(2B1)–P(2B)–O(2B2)	109.2(5)
O(2A3)–P(2A)–C(5A)	108.6(6)	O(2B1)–P(2B)–C(5B)	106.1(6)
O(2B1)–P(2B)–O(2B3)	117.1(5)	O(2B2)–P(2B)–C(5B)	107.1(6)
O(2B3)–P(2B)–O(2B2)	107.5(5)	O(2C1)–P(2C)–O(2C3)	113.3(5)
O(2B3)–P(2B)–C(5B)	109.5(6)	O(2C1)–P(2C)–C(5C)	107.9(6)
O(2C1)–P(2C)–O(2C2)	114.1(5)	O(2C3)–P(2C)–C(5C)	106.6(6)
O(2C2)–P(2C)–O(2C3)	106.7(5)	O(2D1)–P(2D)–O(2D2)	111.5(5)
O(2C2)–P(2C)–C(5C)	107.7(6)	O(2D1)–P(2D)–C(5D)	105.7(6)
O(2D1)–P(2D)–O(2D3)	117.9(6)	O(2D2)–P(2D)–C(5D)	105.7(6)
O(2D3)–P(2D)–O(2D2)	108.0(5)	C(2A)–N(1F)–C(2B)	116.9(10)
O(2D3)–P(2D)–C(5D)	107.4(7)	C(5A)–N(2A)–C(4A)	110.6(10)
C(2D)–N(1E)–C(2C)	118.0(11)	C(3C)–N(2C)–C(5C)	107.9(10)
C(5A)–N(2A)–C(3A)	111.7(11)	C(5C)–N(2C)–C(4C)	113.4(11)
C(3A)–N(2A)–C(4A)	109.7(10)	C(5B)–N(2B)–C(4B)	111.9(10)
C(3C)–N(2C)–C(4C)	106.8(10)	C(5D)–N(2D)–C(3D)	110.7(10)
C(5B)–N(2B)–C(3B)	108.1(9)	C(3D)–N(2D)–C(4D)	108.4(10)
C(3B)–N(2B)–C(4B)	106.5(10)		
C(5D)–N(2D)–C(4D)	108.5(10)		

ative to each other, eventually giving a helical conformation in which they are approximately orthogonal. In a ‘twist–fold’ conformation a slight twisting of the bridgehead units is accompanied by an overall folding of the major ring of the macrocycle so that the pyridine nitrogen atoms and the metal are no longer virtually linear. The conformation of the macrocyclic

framework in [La(H<sub>5</sub>L<sup>2</sup>)] is unlike any other lanthanide complexes with a hexaaza macrocyclic ligand as it shows virtually no twisting (dihedral angle between the dimethylenepyridyl units of 8.5°) nor folding [N(1E)–La–N(1F) 173.3(3)°] so that the lanthanum atom is within 0.01 Å of the best plane through the six macrocycle nitrogen donors; this arrangement is in

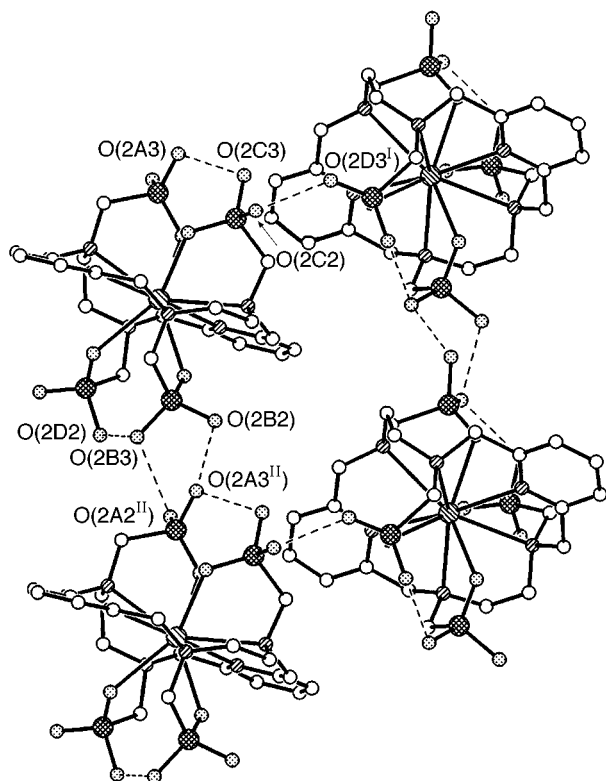


**Fig. 7** Part of the two-dimensional hydrogen-bonded network in the solid-state structure of  $[\text{La}(\text{H}_8\text{L}^2)]$ :  $\text{O}(2\text{A}3) \cdots \text{O}(2\text{C}3)$  2.53,  $\text{O}(2\text{B}3) \cdots \text{O}(2\text{D}2)$  2.57,  $\text{O}(2\text{C}2) \cdots \text{O}(2\text{D}3^{\text{I}})$  2.44,  $\text{O}(2\text{B}2) \cdots \text{O}(2\text{A}3^{\text{II}})$  2.62,  $\text{O}(2\text{B}3) \cdots \text{O}(2\text{A}2^{\text{II}})$  2.61 Å, atoms superscripted I are at  $-0.5 + x, 0.5 + y, 0.5 + z$  and II at  $1 + x, y, z$

direct contrast to the the macrocycle in the related complex  $[\text{Gd}(\text{H}_3\text{L}^3)(\text{NO}_3)]^+$ , which shows a fold-dominated conformation with a  $\text{N}(1\text{E})\text{--Gd--N}(1\text{F})$  angle of only  $146.3(4)^\circ$ .<sup>9</sup> The bond lengths in the co-ordination sphere [ $\text{La--N}(\text{pyridine})$  2.694(10) and 2.731(10),  $\text{La--N}(\text{amine})$  2.780(10)–2.824(10) Å;  $\text{La--O}$  2.517(9)–2.579(8) Å] are comparable to the ranges previously observed for ten-co-ordinated lanthanide complexes;<sup>17</sup> this appears to be the first example of this co-ordination number for a lanthanum hexaaza tetramine macrocycle. With one exception the shortest P–O bond lengths are those involving the donor atoms [1.492–1.506(9) Å]. The terminal bonds  $\text{P}(2\text{A})\text{--O}(2\text{A}3)$  (1.504 Å) and  $\text{P}(2\text{D})\text{--O}(2\text{D}3)$  (1.518 Å) may be assumed to be predominantly unprotonated  $\text{P=O}$  double bonds. Four protons may be assigned to the four longest bonds [range 1.558–1.587(9) Å] and it seems probable that the fifth is disordered over the rather shorter  $\text{P}(2\text{B})\text{--O}(2\text{B}3)$  (1.526) and  $\text{P}(2\text{C})\text{--O}(2\text{C}2)$  bonds (1.534 Å). Very short  $\text{O} \cdots \text{O}$  intra- and inter-molecular distances are consistent with the hydrogen bonding pattern shown in Fig. 7.

## Conclusion

Most aminophosphonates, including  $\text{H}_8\text{L}^5$ ,<sup>18</sup> tend to aggregate and oligomerize in the presence of a metal ion. The present study has demonstrated that the new 18-membered hexaaza macrocyclic ligand with four methylenephosphonate pendants prepared can provide ten donor atoms to encapsulate a fairly large metal ion such as  $\text{La}^{3+}$  in the macrocyclic ring. The complex formed is a discrete monomeric species which is important for its potential applications in biological systems.

## Experimental

### Materials

All reagents and solvents were generally of GPR grade,

obtained from Aldrich Chemical Company and used without further purification, unless otherwise stated. Pyridine-2,6-dicarbaldehyde was prepared by following a literature method<sup>19</sup> with a 87% yield.

### Physical measurements

Microanalyses were performed by the Microanalysis Laboratory and mass spectrometry was carried out by Mass Spectrometry Service of University of North London. Liquid secondary-ion mass spectra (LSIMS) were recorded on a Kratos Profile spectrometer with *m*-nitrobenzyl alcohol as matrix. Fourier-transform IR spectra were recorded as potassium bromide discs for solid samples on a Bio-Rad FTS-40 spectrometer.

### Preparation of $\text{H}_8\text{L}^2$

A solution of aqueous formaldehyde (9.96 g, 119.0 mmol, 37%) was added dropwise to a refluxing solution of  $\text{L}^1$  (5.5 g, 17.0 mmol),<sup>11</sup> phosphorous acid (9.76 g, 119.0 mmol), 35% hydrochloric acid (17.71 g, 170 mmol) and deionised water (10  $\text{cm}^3$ ). The yellow-brown solution was refluxed for 24 h after the addition of the formaldehyde solution. Ethanol (200  $\text{cm}^3$ ) was added dropwise to the cooled solution with stirring until no further white solid precipitated. A white crystalline product (5.28 g, 44%) was obtained by recrystallization of the crude product in boiling aqueous HCl and ethanol. However crystals isolated after this process proved unsuitable for X-ray analysis. Suitable crystals were obtained by recrystallizing a small sample from HCl and  $\text{Pr}^{\text{t}}\text{OH}$ . The product was dried at  $80^\circ\text{C}$  for 24 h, m.p.  $240^\circ\text{C}$  (decomp.) (Found: C, 37.6; H, 5.64; N, 11.9.  $\text{C}_{22}\text{H}_{38}\text{N}_6\text{O}_{12}\text{P}_4$  requires C, 37.6; H, 5.45; N, 12.0%). IR ( $\text{cm}^{-1}$ ): 1598  $\nu[\text{C=N}(\text{py})]$ , 1158,  $\nu(\text{P=O})$  and 1074  $\nu(\text{P-O})$ . LSIMS:  $m/z$  703 (30%),  $[\text{M} + \text{H}]^+$ ; 623 (100%).  $\delta_{\text{C}}(\text{D}_2\text{O}, \text{pD} = 1.58)$  152.1 ( $\text{N}_\alpha\text{C}$ , py), 143.8 ( $\text{N}_\gamma\text{C}$ , py), 127.10 ( $\text{N}_\beta\text{C}$ , py), 63.0 (py- $\text{CH}_2\text{N}$ ), 54.8 ( $\text{NCH}_2\text{CH}_2\text{N}$ ) and 52.0 (d,  $^1J_{\text{CP}}$  143.0 Hz,  $\text{CH}_2\text{P}$ ).  $\delta_{\text{P}}(\text{D}_2\text{O}, \text{pD} 5.0)$  12.39.

### Preparation of lanthanum complex of $\text{H}_8\text{L}^2$

The compound  $\text{La}_2\text{O}_3$  (0.0261 g, 0.080 mmol) was added to a refluxing solution of  $\text{H}_8\text{L}^2$  (0.0755, 0.108 mmol) in water (15  $\text{cm}^3$ ). The mixture was refluxed for 5 h and was filtered hot to remove unreacted  $\text{La}_2\text{O}_3$ . The solvent was removed under reduced pressure to yield a white powder. The product was recrystallised from water-HCl at pH 2.5. Crystals obtained in this way were found to be suitable for X-ray analysis. The product was dried at  $90^\circ\text{C}$  for 30 h. Yield 0.062 g (68.5%), m.p.  $252^\circ\text{C}$  (decomp.) (Found: C, 31.9; H, 4.22; N, 9.95.  $\text{C}_{22}\text{H}_{35}\text{LaN}_6\text{O}_{12}\text{P}_4$  requires C, 31.5; H, 4.21; N, 10.0%). LSIMS:  $m/z$  839,  $[\text{M} + \text{H}]^+$ .  $\delta_{\text{C}}(\text{D}_2\text{O}, \text{pD} 8.2)$  159.1 ( $\text{N}_\alpha\text{C}$ , py), 140.4 ( $\text{N}_\gamma\text{C}$ , py), 123.4 ( $\text{N}_\beta\text{C}$ , py), 66.0 (py- $\text{CH}_2\text{N}$ ), 57.4 ( $\text{NCH}_2\text{CH}_2\text{N}$ ) and 56.5 (d,  $^1J_{\text{CP}}$  125.9 Hz,  $\text{CH}_2\text{P}$ ).  $\delta_{\text{P}}(\text{D}_2\text{O}, \text{pD} 5.4)$  22.92.

### The NMR spectroscopic measurements

Solutions of the ligand (0.020  $\text{mol dm}^{-3}$ ) for NMR pH titrations were made up in  $\text{D}_2\text{O}$  (99.8% from Sigma), and the pD was adjusted with DCl or  $\text{CO}_2$ -free NaOD (Sigma). The final pH was corrected for a deuterium isotope effect by using the equation  $\text{pD} = \text{pH} + 0.4$ .<sup>20</sup> Proton and broadband proton decoupled  $^{13}\text{C}$  and  $^{31}\text{P}$  NMR spectra were obtained at 499.8, 125.7 and 202.3 MHz respectively on a Varian U-500 FT spectrometer;  $^1\text{H}$  shifts were referenced to internal HOD at 4.75 ppm and  $^{31}\text{P}$  shifts were referenced to external 85%  $\text{H}_3\text{PO}_4$ .

### Crystallography

**X-Ray structural analyses.** Intensity data for  $\text{H}_8\text{L}^2$  and  $[\text{La}(\text{H}_8\text{L}^2)]$  were collected on a Siemens P4 diffractometer, using

**Table 3** Crystal data and structure refinement for H<sub>8</sub>L<sup>2</sup>·12H<sub>2</sub>O and [La(H<sub>5</sub>L<sup>2</sup>)]

	H <sub>8</sub> L <sup>2</sup> ·12H <sub>2</sub> O	[La(H <sub>5</sub> L <sup>2</sup> )]
Empirical formula	C <sub>22</sub> H <sub>62</sub> N <sub>6</sub> O <sub>24</sub> P <sub>4</sub>	C <sub>22</sub> H <sub>35</sub> LaN <sub>6</sub> O <sub>12</sub> P <sub>4</sub>
<i>M</i>	918.66	838.03
Crystal system	Orthorhombic	Monoclinic
Space group	<i>Aba2</i>	<i>P2<sub>1</sub>/n</i>
<i>a</i> /Å	13.893(5)	11.302 8(13)
<i>b</i> /Å	27.578(6)	16.069(2)
<i>c</i> /Å	23.088(8)	17.0410(9)
β/°	—	104.515(8)
<i>U</i> /Å <sup>3</sup> , <i>Z</i>	8846(5), 8	2996.2(5), 4
<i>D<sub>c</sub></i> /g cm <sup>-3</sup>	1.380	1.858
μ/mm <sup>-1</sup>	0.256	13.685
<i>T</i> /K	293(2)	213(2)
λ/Å	0.710 73	1.541 78
<i>F</i> (000)	3904	1688
θ Range/°	1.48–22.00	3.84–56.73
<i>hkl</i> Ranges	–1 to 16, –32 to 1, –1 to 27	–12 to 11, 0–17, 0–18
Independent reflections, <i>R<sub>int</sub></i>	3405, 0.1068	4008, 0.0756
Data, restraints, parameters	2528, 50, 368	4008, 0, 406
Goodness of fit <i>S</i> on <i>F</i> <sup>2</sup>	1.017	1.042
Final <i>R</i> indices <i>R</i> <sub>1</sub> , <i>wR</i> <sub>2</sub> [ <i>I</i> > 2σ( <i>I</i> )]	0.0939, 0.2167	0.0730, 0.1769
(all data)	0.2067, 0.2998	0.1033, 0.1997
Largest difference peak and hole/e Å <sup>-3</sup>	0.454 and –0.456	2.406 and –2.025

$S = [\sum w(F_o^2 - F_c^2)^2 / (n - p)]^{1/2}$ , where *n* = number of reflections and *p* = total number of parameters;  $R_1 = \sum ||F_o| - |F_c|| / \sum |F_o|$ ,  $wR_2 = \sum [w(F_o^2 - F_c^2)^2] / \sum [w(F_o^2)^2]$ ,  $w^{-1} = [\sigma^2(F_o^2) + (tP)^2] \{t = 0.1270 \text{ for H}_8\text{L}^2 \text{ and } 0.1129 \text{ for [La(H}_5\text{L}^2)]\}$ , where  $P = [\max(F_o^2, 0) + 2(F_c^2)]/3$ .

ω–2θ scans and graphite-monochromated Cu-Kα radiation for [La(H<sub>5</sub>L<sup>2</sup>)] and Mo-Kα radiation for H<sub>8</sub>L<sup>2</sup>. Details of the crystal data, data collection and refinement are summarised in Table 3. During data collection, three standard reflections measured after every 97 reflections showed no significant variation in intensity; the data were corrected for Lorentz and polarisation factors.

**Structure solution and refinement.**<sup>21</sup> The structure of the ligand H<sub>8</sub>L<sup>2</sup> was solved by direct methods and for [La(H<sub>5</sub>L<sup>2</sup>)] the position of the lanthanum atom was deduced by the Patterson method; the remaining non-hydrogen atoms for both structures were located from subsequent Fourier-difference syntheses. In H<sub>8</sub>L<sup>2</sup>, a large number of residual maxima in a Fourier-difference map were assigned as water molecules, eight of full occupancy, four half occupancy and eight quarter occupancy, giving a total of twelve water molecules per asymmetric unit. An empirical absorption correction was applied to the data of [La(H<sub>5</sub>L<sup>2</sup>)] after initial refinement with isotropic displacement parameters for all atoms.<sup>22</sup> All the non-hydrogen atoms in the complex [La(H<sub>5</sub>L<sup>2</sup>)], and the phosphorus and full occupancy oxygen atoms in H<sub>8</sub>L<sup>2</sup>, were assigned anisotropic displacement parameters and refined using a full-matrix least-squares procedure, based on *F*<sup>2</sup>. For H<sub>8</sub>L<sup>2</sup> chemically equivalent bond lengths in the macrocyclic backbone were constrained to be equal within an estimated standard deviation (e.s.d.) of 0.03 Å, and the pyridine rings were constrained to be flat. For both structures the carbon bonded hydrogen atoms were placed in an idealised geometry and were allowed to ride on their parent atom, with those of the pyridyl assigned isotropic displacement parameters equal to 1.2 *U*<sub>eq</sub> of the parent carbon atoms and those of the methylene and ethyl groups 1.5 *U*<sub>eq</sub>. A final Fourier-difference map of [La(H<sub>5</sub>L<sup>2</sup>)] showed residual electron density of ca. 2.5 e Å<sup>-3</sup> in the vicinity of the metal atom.

CCDC reference number 186/648.

## Acknowledgements

We thank the EPSRC for a studentship (to T. M. W.) and for use of the Chemical Database Service at Daresbury. C. F. G. C. G. thanks Junta Nacional de Investigação Científica

e Tecnológica, Portugal (grant Praxis XXI 2/2.2/SAU/1194/95) for financial support.

## References

- M. F. Loncin, J. F. Desreux and E. Merciny, *Inorg. Chem.*, 1986, **25**, 2646.
- A. D. Sherry, J. Ren, J. Huskens, E. Brücher, E. Tóth, C. F. G. C. Geraldès, M. M. C. A. Castro and W. P. Cacheris, *Inorg. Chem.*, 1996, **35**, 4604.
- C. F. G. C. Geraldès, A. D. Sherry and G. E. Kiefer, *J. Magn. Reson.*, 1992, **97**, 290.S.
- S. Aime, M. Botta, E. Terreno, P. L. Anelli and F. Uggeri, *Magn. Reson. Med.*, 1993, **30**, 583.
- L. R. Dick, C. F. G. C. Geraldès, A. D. Sherry, C. W. Gray and D. M. Gray, *Biochemistry*, 1989, **28**, 7896.
- D. W. Swinkels, J. P. M. van Duynhoven, C. W. Hilbers and G. I. Tesser, *Recl. Trav. Chim. Pays-Bas*, 1991, **110**, 124.
- N. Bansal, M. J. Germann, V. Seshan, G. T. Shires III, C. R. Malloy and A. D. Sherry, *Biochemistry*, 1993, **32**, 5638.
- V. Seshan, M. J. Germann, P. Preisig, C. R. Malloy, A. D. Sherry and N. Bansal, *Magn. Reson. Med.*, 1995, **34**, 25.
- S. W. A. Bligh, N. Choi, W. J. Cummins, E. G. Evagorou, J. D. Kelly and M. McPartlin, *J. Chem. Soc., Dalton Trans.*, 1993, 3829.
- C. F. G. C. Geraldès, A. D. Sherry and W. P. Cacheris, *Inorg. Chem.*, 1989, **28**, 3336.
- G. L. Rothermel, jun., L. Miao, A. L. Hill and S. C. Jackels, *Inorg. Chem.*, 1992, **31**, 4854.
- J. L. Sudmeier and C. N. Reilley, *Anal. Chem.*, 1964, **36**, 1698.
- W. Clegg, P. B. Iveson and J. C. Lockhart, *J. Chem. Soc., Dalton Trans.*, 1992, 3291.
- I. Lázár, D. C. Hrnčir, W.-D. Kim, G. E. Kiefer and A. D. Sherry, *Inorg. Chem.*, 1992, **31**, 4422.
- G. V. Polyanchuk, L. M. Shkol'nikova, M. V. Rudomino, N. M. Dyatlova and S. S. Makarevich, *Zh. Strukt. Khim.*, 1985, **26**, 109.
- N. Y. C. Choi, Ph.D. Thesis, University of North London, 1996.
- V. Alexander, *Chem. Rev.*, 1995, **95**, 273.
- C. F. G. C. Geraldès, R. D. Brown III, W. P. Cacheris, S. H. Koenig, A. D. Sherry and M. Spiller, *Magn. Reson. Med.*, 1989, **9**, 94.
- N. W. Alcock, R. G. Kingston, P. Moore and C. Pierpoint, *J. Chem. Soc., Dalton Trans.*, 1984, 1937.
- P. K. Glasoe and F. A. Long, *J. Phys. Chem.*, 1960, **64**, 188.
- SHELXTL, PC version 5.03, Siemens Analytical Instruments Inc., Madison, WI, 1994.
- S. R. Parkin, B. Moezzi and H. Hope, XABS 2, *J. Appl. Crystallogr.*, 1995, **28**, 53.

Received 28th May 1997; Paper 7/03678G